

# A Josephson–SQUID Barrier-Clock Diagnostic for the Residual Clock–Energy Framework

Gauge-Invariant Phase Tension, Tunneling Opacity,  
Phase Noise, and Frequency-Shift Covariance

Byoungwoo Lee  
Independent Researcher  
Daejeon, Republic of Korea

Version v0.5r2 – Executable Diagnostic I – April 2026

## Abstract

This review-integrated note gives the first device-facing executable diagnostic for the Residual Clock–Energy framework. It follows the public protocol draft *Prediction and Discriminating Experiments for the Residual Clock–Energy Framework* and narrows the five-channel prediction program to one concrete laboratory channel: a Josephson/SQUID barrier-clock diagnostic. No empirical detection is claimed, no new Josephson law is proposed, and no replacement of standard superconducting-device physics is intended. The target is a covariance diagnostic built on the ordinary Josephson relations, SQUID flux modulation, WKB tunneling opacity, and phase-noise bookkeeping.

The diagnostic starts from the gauge-invariant superconducting phase difference

$$\phi = \varphi_1 - \varphi_2 - \frac{2\pi}{\Phi_0} \int_1^2 A \cdot d\ell,$$

which is compared with the residual clock one-form  $\alpha = d\Phi - A$ . A flux-bias variable  $u = \Phi_{\text{ext}}/\Phi_0$  controls a toy residual drive

$$\mathcal{R}_J(u) = r_0 \sin^2(\pi u),$$

and the proposed observable export is

$$u \mapsto \left( I_c(u), \Gamma_\phi(u), \frac{\delta\nu_{\text{osc}}}{\nu_{\text{osc}}}(u), S_{\phi\phi}(\omega; u) \right).$$

The residual hypothesis is not that any one of these quantities is anomalous. It is that the baseline-subtracted non-current observables show a common morphology controlled by the same residual drive, after nuisance controls for heating, electromagnetic pickup, flux noise, bias drift, device aging, and technical phase noise.

Version v0.5r2 includes an executable toy flux grid, plotted residual covariance targets, an RCSJ-style phase-dynamics baseline, baseline-subtracted observables, an explicit  $H_0/H_1$  covariance diagnostic, a tunneling-time taxonomy table, nuisance-morphology comparisons, a morphology-score admission rule, a boundary-layer tunneling-clock profile, a nuisance-control table, and a falsifiability ledger. The ideal toy curves are positive-control injections, not empirical support; their purpose is to define the morphology that an experiment would attempt to recover after nuisance projection. The intended use is methodological: the note provides a reproducible diagnostic template for superconducting phase devices, SQUID metrology, tunnel-barrier screening, and cryogenic phase-noise classification.

## Contents

### 1 Introduction

3

<b>2</b>	<b>Gauge-Invariant Phase Difference and Residual One-Form</b>	<b>3</b>
<b>3</b>	<b>Standard Josephson/SQUID Baseline</b>	<b>4</b>
3.1	Minimal phase-dynamics and noise baseline . . . . .	5
<b>4</b>	<b>Residual Clock Deformation of Josephson Observables</b>	<b>5</b>
<b>5</b>	<b>Barrier-Clock Tunneling Layer</b>	<b>6</b>
<b>6</b>	<b>Executable Toy Flux Grid</b>	<b>8</b>
6.1	Nuisance morphology comparison . . . . .	8
<b>7</b>	<b>Covariance Score and Residual Admissibility</b>	<b>9</b>
<b>8</b>	<b>Nuisance-Control and Error Budget</b>	<b>11</b>
<b>9</b>	<b>Falsifiability Ledger</b>	<b>12</b>
<b>10</b>	<b>Application Outlook</b>	<b>13</b>
<b>11</b>	<b>Conclusion</b>	<b>14</b>
<b>A</b>	<b>Toy Model Parameters</b>	<b>15</b>
<b>B</b>	<b>Pseudocode</b>	<b>15</b>
<b>C</b>	<b>Relation to the v0.4r1 Public Protocol Note</b>	<b>15</b>
<b>D</b>	<b>Reproducibility Bundle Contents</b>	<b>16</b>

# 1 Introduction

The Residual Clock–Energy framework organizes phase tension, structural lapse, operational time, and generator cost through the schematic chain

$$\alpha = d\Phi - A \longrightarrow R_\alpha \longrightarrow L_\alpha \longrightarrow T \longrightarrow K_T. \quad (1)$$

The public protocol note associated with the framework proposed five falsifiable channels: CMB transfer morphology, laboratory phase-clock response, microscopic tunneling, lattice lapse-map structure, and black-hole boundary-scar scaling [1]. That protocol note deliberately avoided claiming an empirical detection. Its role was to ask what the framework should predict if it is to become experimentally constrained.

The present v0.5r2 note is the first executable follow-up. It chooses one channel – Josephson/SQUID phase-coherent devices with a tunneling barrier – and converts the protocol-level idea into a toy calculation and null-test ledger. The motivation is direct. A Josephson device already contains a gauge-invariant phase difference, a tunnel barrier, flux modulation, critical-current response, phase noise, and oscillator-frequency readout. Therefore it is a natural device-level arena in which to test whether a residual phase-clock drive can be operationally separated from ordinary nuisance mechanisms.

The central claim posture is conservative:

- standard Josephson and SQUID physics are the baseline;
- WKB tunneling opacity is recovered as the transmission baseline;
- no experimental confirmation of the Residual Clock–Energy framework is asserted;
- the proposed object is a covariance diagnostic, not a new superconducting-device law.

In particular, a modulation of the critical current alone is not a residual-clock signature. Critical-current modulation is already the ordinary SQUID response. A positive residual interpretation would require a multi-observable covariance pattern among baseline-subtracted phase dephasing, frequency shift, phase-noise spectrum, and residual current correction, all tied to a declared residual drive.

The paper is organized as follows. [Section 2](#) connects the gauge-invariant superconducting phase difference to the residual one-form. [Section 3](#) recalls the standard Josephson/SQUID baseline. [Section 4](#) defines the residual clock deformation of observable channels. [Section 5](#) adds the barrier-clock tunneling layer and the phase-time observable. [Section 6](#) gives the executable toy flux grid and plots. [Section 7](#) defines morphology scores and residual admissibility. [Section 8](#) gives the nuisance-control and error-budget protocol. [Section 9](#) states the falsifiability ledger. [Section 10](#) discusses application relevance. Appendices record toy parameters, pseudocode, and the relation to the v0.4r1 protocol note.

## 2 Gauge-Invariant Phase Difference and Residual One-Form

A superconducting weak link is a natural setting for phase-based diagnostics. Let  $\varphi_1$  and  $\varphi_2$  be the phases of the superconducting order parameter on the two sides of a junction. The gauge-invariant phase difference is

$$\phi = \varphi_1 - \varphi_2 - \frac{2\pi}{\Phi_0} \int_1^2 A \cdot d\ell, \quad \Phi_0 = \frac{h}{2e}. \quad (2)$$

This is the standard phase variable entering the Josephson relations [3, 4, 5]. In a SQUID loop, the external flux controls the accumulated gauge phase and hence the interference of two junction paths.

The Residual Clock–Energy framework uses a residual phase-tension one-form

$$\alpha = d\Phi - A. \quad (3)$$

In this note, (3) is not introduced as a new electromagnetic field. It is a residual bookkeeping object measuring mismatch between phase evolution and gauge compensation. The Josephson/SQUID platform is useful because this bookkeeping object has a natural operational proxy: the flux-controlled gauge-invariant phase around the loop.

Let

$$u = \frac{\Phi_{\text{ext}}}{\Phi_0} \quad (4)$$

be the normalized external flux. The residual phase-clock drive is represented by a nonnegative scalar functional of the residual one-form over the active junction or SQUID loop region.

**Definition 2.1** (Josephson residual phase-clock drive). For a flux-biased Josephson/SQUID platform, a residual phase-clock drive is a nonnegative function

$$\mathcal{R}_J(u) = \lambda_J \left\langle |\alpha(u)|^2 \right\rangle_{\text{junction}}, \quad \lambda_J \geq 0. \quad (5)$$

For the first executable toy pass, we use the symmetric normalized drive

$$\mathcal{R}_J(u) = r_0 \sin^2(\pi u), \quad 0 \leq u \leq 1, \quad 0 < r_0 \ll 1. \quad (6)$$

The choice (6) is not a microscopic derivation. It is a controlled first diagnostic morphology. It has the expected periodicity in normalized flux, it is nonnegative, and it peaks where the ideal symmetric SQUID critical current is suppressed. More elaborate versions may include asymmetry, trapped vortices, junction nonuniformity, or spectral filters. The purpose of v0.5 is to make the first executable residual-covariance test explicit.

**Remark 2.2** (Why Josephson/SQUID rather than a generic oscillator?). A generic oscillator can test frequency drift or phase noise, but it does not naturally expose a gauge-invariant phase difference and a tunneling barrier in the same device. A Josephson/SQUID device does. This makes it a bridge between the residual one-form  $\alpha = d\Phi - A$ , phase-clock response, and tunneling opacity.

### 3 Standard Josephson/SQUID Baseline

The residual diagnostic must be built on standard device physics. The dc Josephson relation is

$$I_s = I_c \sin \phi, \quad (7)$$

and the ac Josephson relation is

$$V = \frac{\hbar}{2e} \dot{\phi}. \quad (8)$$

For a symmetric dc SQUID with negligible loop inductance and identical junctions, the ideal critical-current modulation is

$$I_c^{(0)}(u) = 2I_{c0} |\cos(\pi u)|. \quad (9)$$

In a real device, junction asymmetry and finite visibility smooth the ideal nodes. A convenient toy baseline is

$$I_c^{(0)}(u) = 2I_{c0} \sqrt{\cos^2(\pi u) + \varepsilon_{\text{asym}}^2}, \quad 0 < \varepsilon_{\text{asym}} \ll 1. \quad (10)$$

This smoothing is not intended as a full device model. It prevents the toy diagnostic from overemphasizing a cusp at the ideal SQUID node.

The baseline model also includes ordinary dephasing, technical phase noise, and oscillator drift:

$$\Gamma_{\phi}^{(0)}(u) = \Gamma_0 + \Gamma_{\text{nuis}}(u), \quad (11)$$

$$\left(\frac{\delta\nu_{\text{osc}}}{\nu_{\text{osc}}}\right)^{(0)}(u) = \Delta_{\text{nuis}}(u), \quad (12)$$

$$S_{\phi\phi}^{(0)}(\omega; u) = S_{\text{th}}(\omega; u) + S_{1/f}(\omega; u) + S_{\text{tech}}(\omega; u). \quad (13)$$

The residual diagnostic does not deny these nuisance terms. It requires that residual admission be made only after these ordinary channels are controlled, reversed, subtracted, or bounded.

### 3.1 Minimal phase-dynamics and noise baseline

For device-facing readers it is useful to place the diagnostic next to the minimal resistively and capacitively shunted junction (RCSJ) phase dynamics. A standard schematic form is

$$C \frac{\Phi_0}{2\pi} \ddot{\phi} + \frac{1}{R} \frac{\Phi_0}{2\pi} \dot{\phi} + I_c \sin \phi = I_b + I_n(t), \quad (14)$$

where  $C$  is the junction capacitance,  $R$  is the shunt resistance,  $I_b$  is the bias current, and  $I_n(t)$  denotes ordinary current noise. Equivalently, after nondimensionalization one may write

$$\ddot{\phi} + \gamma_J \dot{\phi} + \omega_J^2 \sin \phi = \eta_b + \xi(t). \quad (15)$$

The residual model is not a substitute for (14) or (15). Its target is the residual left after a baseline phase-dynamics and noise model has been fitted. In other words, Residual Clock–Energy contributes a covariance layer for baseline-subtracted residuals, not a replacement dynamics for Josephson junctions [7, 8, 9].

**Diagnostic 3.1** (Baseline recovery requirement). A Josephson/SQUID barrier-clock diagnostic is admissible only if the zero-residual limit recovers the standard Josephson relations (7)–(8), the baseline SQUID flux modulation (10), and the declared ordinary noise model. Residual terms are interpreted only as small deformations around this baseline.

## 4 Residual Clock Deformation of Josephson Observables

The residual drive (6) induces a structural lapse

$$L_J(u) = \exp\{-\mathcal{R}_J(u)\}. \quad (16)$$

In the small-residual regime,

$$L_J(u) = 1 - \mathcal{R}_J(u) + O(\mathcal{R}_J(u)^2). \quad (17)$$

The simplest observable export is a vector

$$u \mapsto \left( I_c(u), \Gamma_{\phi}(u), \frac{\delta\nu_{\text{osc}}}{\nu_{\text{osc}}}(u), S_{\phi\phi}(\omega; u) \right). \quad (18)$$

Each component has a standard baseline plus a residual correction. For scoring, the raw observables are converted into a baseline-subtracted vector

$$\mathbf{y}(u) = \left( \frac{\Delta I_c(u)}{I_c^{(0)}(u)}, \Delta \Gamma_{\phi}(u), -\frac{\delta\nu_{\text{osc}}}{\nu_{\text{osc}}}(u), \Delta S_{\phi\phi}(\omega_0; u) \right), \quad (19)$$

where

$$\Delta I_c(u) := I_c(u) - I_c^{(0)}(u), \quad (20)$$

$$\Delta \Gamma_\phi(u) := \Gamma_\phi(u) - \Gamma_\phi^{(0)}(u), \quad (21)$$

$$\Delta S_{\phi\phi}(\omega_0; u) := S_{\phi\phi}(\omega_0; u) - S_{\phi\phi}^{(0)}(\omega_0; u). \quad (22)$$

This convention prevents the ordinary SQUID interference envelope from being misread as a residual-clock signal. In experimental use, the ratio channel  $\Delta I_c/I_c^{(0)}$  should be masked or down-weighted near SQUID nodes where  $I_c^{(0)}(u) \leq I_{\min}$ . In those windows, absolute residuals  $\Delta I_c(u)$  or covariance-weighted current residuals are preferable to a raw ratio, because the denominator can amplify ordinary readout noise.

For the frequency shift, clock suppression gives

$$\frac{\delta \nu_{\text{osc}}}{\nu_{\text{osc}}}(u) = -\lambda_\nu \mathcal{R}_J(u) + \Delta_{\text{nuis}}(u) + O(\mathcal{R}_J^2). \quad (23)$$

For the dephasing rate,

$$\Gamma_\phi(u) = \Gamma_0 + \lambda_\Gamma \mathcal{R}_J(u) + \Gamma_{\text{nuis}}(u) + O(\mathcal{R}_J^2). \quad (24)$$

For the phase-noise spectrum at a fixed readout band,

$$S_{\phi\phi}(\omega; u) = S_{\phi\phi}^{(0)}(\omega; u) + \lambda_S F_S(\omega) \mathcal{R}_J(u) + O(\mathcal{R}_J^2). \quad (25)$$

For the critical current, the residual term is included only as a small correction to the ordinary SQUID interference envelope:

$$I_c(u) = I_c^{(0)}(u) [1 - \lambda_I \mathcal{R}_J(u)] + O(\mathcal{R}_J^2). \quad (26)$$

This distinction is crucial. The raw current modulation  $I_c^{(0)}(u)$  is not evidence for a residual clock sector; it is ordinary SQUID physics. Only baseline-subtracted residual channels can enter the covariance test.

**Diagnostic 4.1** (Residual covariance target). The Josephson/SQUID residual-clock signature is the common morphology

$$\mathcal{R}_J(u) \mapsto \left( \Delta I_c(u), \Delta \Gamma_\phi(u), -\frac{\delta \nu_{\text{osc}}}{\nu_{\text{osc}}}(u), S_{\phi\phi}^{\text{res}}(\omega_0; u) \right), \quad (27)$$

where

$$\Delta I_c(u) := I_c(u) - I_c^{(0)}(u), \quad (28)$$

$$\Delta \Gamma_\phi(u) := \Gamma_\phi(u) - \Gamma_0 - \Gamma_{\text{nuis}}(u), \quad (29)$$

$$S_{\phi\phi}^{\text{res}}(\omega_0; u) := S_{\phi\phi}(\omega_0; u) - S_{\phi\phi}^{(0)}(\omega_0; u). \quad (30)$$

A current-only modulation is not a residual-clock signature.

## 5 Barrier-Clock Tunneling Layer

A Josephson junction is also a tunneling device. The tunneling layer of the diagnostic must first recover the standard WKB opacity and transmission law. For a one-dimensional barrier  $V(x) > E$  on  $[x_1, x_2]$ , define

$$\kappa(x) = \frac{\sqrt{2m(V(x) - E)}}{\hbar}, \quad (31)$$

Table 1: Tunneling-time observable taxonomy for the v0.5r2 diagnostic.

Observable	Schematic definition	Role in this note
Phase time / Wigner–Smith proxy	$\tau_\varphi(E) = \hbar \partial_E \arg t(E)$	primary first-pass traversal-time observable
Dwell time	barrier probability divided by incident flux	secondary cross-check for barrier support
Larmor-clock time	spin-precession clock in a weak magnetic field	future experimental cross-check
Weak-measurement time	weak-value or postselected timing protocol	not used in the v0.5r2 toy calculation
Detector response time	apparatus-dependent arrival or switching response	nuisance-sensitive diagnostic, not a primary clock

and

$$\mathcal{R}_B = \int_{x_1}^{x_2} \kappa(x) \, dx. \quad (32)$$

The WKB transmission baseline is

$$\mathcal{T} \sim e^{-2\mathcal{R}_B}. \quad (33)$$

In a real Josephson junction,  $\mathcal{R}_B$  should be interpreted as an effective opacity ledger rather than as a literal single-particle WKB parameter unless the junction model explicitly supports that reduction. This caution is important because Cooper-pair tunneling, oxide-barrier defects, and microscopic junction transparency need not reduce to a single one-dimensional opacity integral.

The first public implementation uses the phase-time or Wigner–Smith proxy as the primary traversal-time observable:

$$\tau_\varphi(E) = \hbar \frac{\partial}{\partial E} \arg t(E), \quad (34)$$

where  $t(E)$  is the complex transmission amplitude. Dwell time and Larmor-clock time are treated as secondary cross-checks [11, 12, 13]. This convention reduces the ambiguity of the phrase “tunneling time” while keeping the broader tunneling-time literature visible.

The residual barrier-clock layer does not replace (33). It introduces a clock-support profile inside the barrier. Define the boundary-layer opacity depth

$$\rho_B(x) = \min \left\{ \int_{x_1}^x \kappa(y) \, dy, \int_x^{x_2} \kappa(y) \, dy \right\}, \quad (35)$$

and the corresponding lapse profile

$$L_{\text{tun}}(x) = e^{-\rho_B(x)}. \quad (36)$$

For a uniform barrier on  $[0, a]$  with constant  $\kappa$ , one obtains

$$\int_0^a e^{-\rho_B(x)} \, dx = \frac{2}{\kappa} \left( 1 - e^{-\kappa a/2} \right). \quad (37)$$

Thus in the opaque limit  $\kappa a \gg 1$ ,

$$\Delta T_{\text{op}}^{\text{BL}} \propto \int_0^a e^{-\rho_B(x)} \, dx \longrightarrow \frac{2}{\kappa}. \quad (38)$$

This is not presented as a solution of the Hartman-effect problem. It is a boundary-layer operational-clock saturation proxy that can be compared with a declared phase-time observable.

**Diagnostic 5.1** (Barrier-clock covariance map). The tunneling part of the diagnostic is the opacity-linked map

$$\mathcal{R}_B \mapsto \left( \mathcal{T}, \tau_\varphi, S_{\phi\phi}^{\text{res}}, \Gamma_\phi \right), \quad (39)$$

with (33) as the baseline and (36)–(38) as a residual operational-clock proxy. The diagnostic succeeds only if the declared time/noise/dephasing observables co-vary with opacity after ordinary barrier and heating controls.

## 6 Executable Toy Flux Grid

This section is the difference between the present v0.5r2 note and the earlier protocol layer. The toy model is not a data fit. It is a reproducible diagnostic grid showing what a residual phase-clock covariance pattern would look like before experimental noise and calibration are added.

The ideal residual-only curves in this section should be read as positive-control injections. Their purpose is to define the morphology that a real experiment would attempt to recover after nuisance projection, not to demonstrate empirical support. In particular, a high morphology score in the synthetic residual channels is expected by construction and should be interpreted as a calibration target for the diagnostic, not as evidence for the framework.

Let

$$u_i = \frac{i}{N}, \quad i = 0, 1, \dots, N, \quad N = 200. \quad (40)$$

Use the toy parameter set

$$r_0 = 0.05, \quad \varepsilon_{\text{asym}} = 0.05, \quad \lambda_I = 0.2, \quad \lambda_\nu = \lambda_\Gamma = \lambda_S = 1. \quad (41)$$

The residual drive is

$$\mathcal{R}_J(u) = r_0 \sin^2(\pi u). \quad (42)$$

The baseline critical current is normalized as

$$\hat{I}_c^{(0)}(u) = \frac{\sqrt{\cos^2(\pi u) + \varepsilon_{\text{asym}}^2}}{\sqrt{1 + \varepsilon_{\text{asym}}^2}}, \quad (43)$$

and the residual-deformed current is

$$\hat{I}_c(u) = \hat{I}_c^{(0)}(u) [1 - \lambda_I \mathcal{R}_J(u)]. \quad (44)$$

The non-current residual observables are

$$\Gamma_\phi(u) = \Gamma_0 + \lambda_\Gamma \mathcal{R}_J(u), \quad (45)$$

$$-\frac{\delta\nu_{\text{osc}}}{\nu_{\text{osc}}}(u) = \lambda_\nu \mathcal{R}_J(u), \quad (46)$$

$$S_{\phi\phi}^{\text{res}}(\omega_0; u) = \lambda_S F_S(\omega_0) \mathcal{R}_J(u). \quad (47)$$

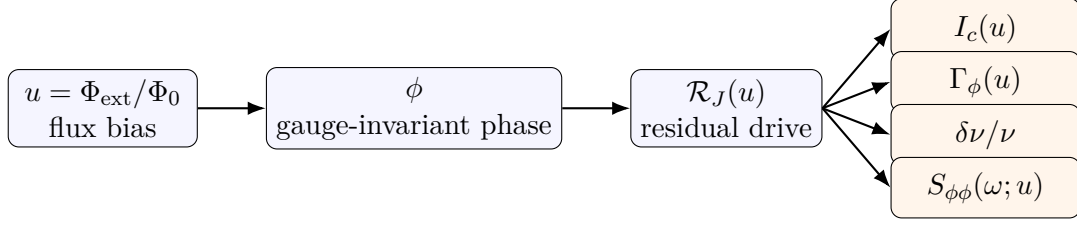
For the displayed toy grid we set  $\Gamma_0 = 1$  and  $F_S(\omega_0) = 1$ .

### 6.1 Nuisance morphology comparison

A toy residual plot is not enough unless it is compared with nuisance morphologies. In the v0.5r2 grid we therefore include three schematic controls:

$$H(u) = h_0 + h_1 \left( \hat{I}_c^{(0)}(u) \right)^2, \quad (48)$$





diagnostic target: common morphology after nuisance projection

Figure 1: Device-level diagnostic logic. Flux bias controls the gauge-invariant phase and the declared residual drive. The residual hypothesis is admitted only if multiple baseline-subtracted observables share the same residual morphology.

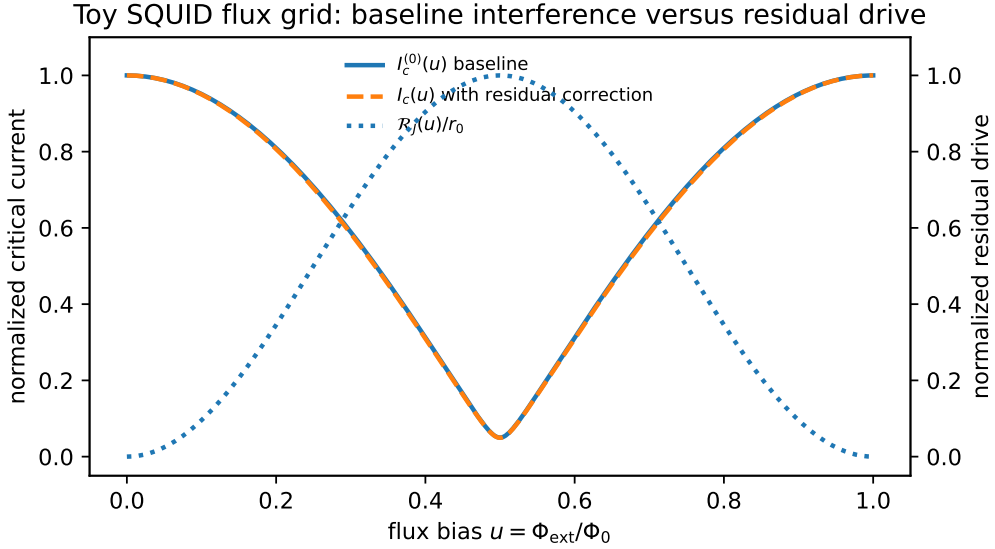


Figure 2: Toy SQUID flux grid. The raw critical-current modulation is dominated by the ordinary SQUID interference baseline. The residual drive  $\mathcal{R}_J(u)$  is therefore not inferred from current modulation alone.

$$D(u) = u - \langle u \rangle, \quad (49)$$

$$Q(u) = q_1 \sin(4\pi u) + q_2 \cos(6\pi u). \quad (50)$$

The first represents a power/heating-like morphology, the second a sweep-order or bias drift proxy, and the third a residual-insensitive dummy channel. None of these should be admitted as a residual-clock signal merely because it varies with flux.

## 7 Covariance Score and Residual Admissibility

A visual covariance plot is not enough. The diagnostic needs a score that can be applied to real data after nuisance projection. The statistical distinction is between an ordinary- nuisance null model

$$H_0 : \quad \mathbf{y}(u_i) = \mathbf{n}(u_i), \quad (51)$$

and a residual-covariance alternative

$$H_1 : \quad \mathbf{y}(u_i) = \beta g(u_i) + \mathbf{n}(u_i), \quad (52)$$

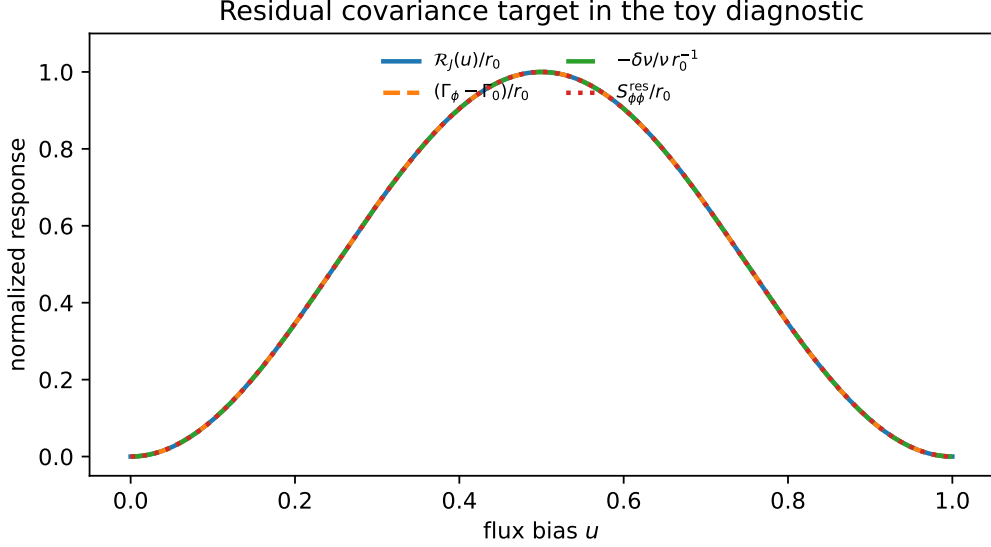


Figure 3: Residual covariance target in the toy diagnostic. In the ideal residual-only model, the non-current channels  $\Delta\Gamma_\phi$ ,  $-\delta\nu/\nu$ , and  $S_{\phi\phi}^{\text{res}}$  share the same morphology as  $\mathcal{R}_J(u)$ . This plot is a positive-control diagnostic target, not a data claim or empirical support.

where  $\mathbf{y}$  is the baseline-subtracted vector in (19),  $g$  is the centered residual design vector,  $\beta$  is a channel-response vector, and  $\mathbf{n}$  contains ordinary nuisance residues after controls. A residual claim is meaningful only if  $H_1$  improves the morphology fit without violating the nuisance ledger.

Let  $g_i$  be the centered residual design vector

$$g_i = \mathcal{R}_J(u_i) - \frac{1}{N+1} \sum_{m=0}^N \mathcal{R}_J(u_m). \quad (53)$$

For a baseline-subtracted observable  $y_{k,i} = y_k(u_i)$ , define the one-parameter projection coefficient

$$\hat{a}_k = \frac{\sum_i g_i y_{k,i}}{\sum_i g_i^2}. \quad (54)$$

Define the morphology score

$$M_k = \frac{|\sum_i g_i y_{k,i}|}{(\sum_i g_i^2)^{1/2} (\sum_i y_{k,i}^2)^{1/2}}. \quad (55)$$

The ideal residual-only model gives  $M_k = 1$  for the non-current residual channels because those channels are generated from the design morphology. This is a positive-control sanity check. Real experiments require thresholding after error modeling, nuisance projection, and synthetic-noise injection. In this note we use a toy threshold

$$M_{\min} = 0.85 \quad (56)$$

only as an illustration.

**Diagnostic 7.1** (Residual-admission rule). A Josephson/SQUID residual-clock interpretation is admitted only if at least two non-current channels satisfy

$$M_k \geq M_{\min}, \quad k \in \{\Delta\Gamma_\phi, -\delta\nu_{\text{osc}}/\nu_{\text{osc}}, S_{\phi\phi}^{\text{res}}\}, \quad (57)$$

after declared nuisance controls. Raw current modulation is not sufficient.

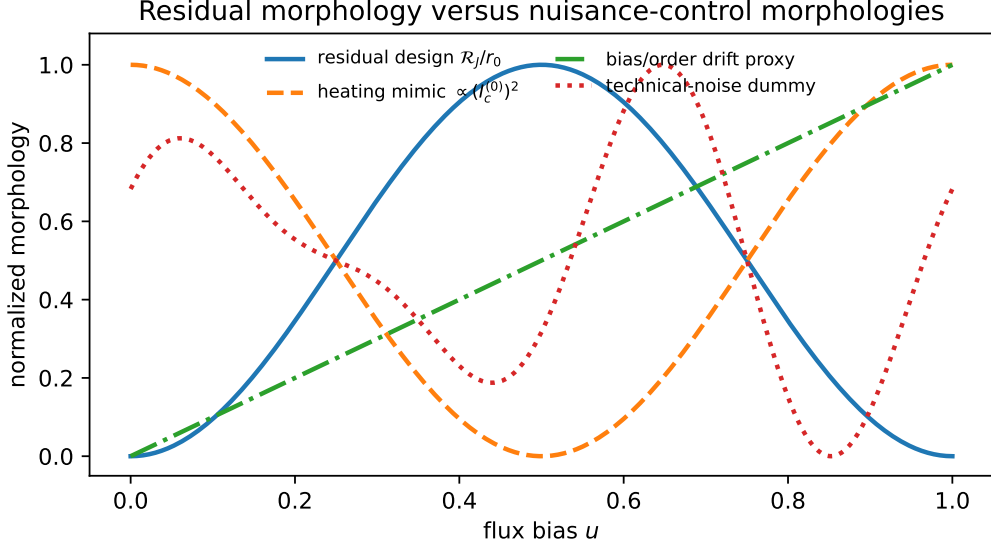


Figure 4: Residual morphology versus nuisance-control morphologies. The purpose is not to model all experimental artifacts, but to show that the residual design vector must compete against declared alternatives such as heating, bias drift, and dummy technical noise.

A high morphology score in a positive-control toy injection is not evidence for the physical framework. It only confirms that the analysis pipeline can recover the morphology it was designed to recover. Evidence-facing use would require blind or synthetic-noise recovery, nuisance projection, and device-calibrated uncertainty estimates.

The score (55) can be generalized by replacing the Euclidean inner product with a covariance-weighted inner product. If  $\Sigma_k$  is the covariance matrix for a channel, one may use

$$M_k^{(\Sigma)} = \frac{|g^T \Sigma_k^{-1} y_k|}{(g^T \Sigma_k^{-1} g)^{1/2} (y_k^T \Sigma_k^{-1} y_k)^{1/2}}. \quad (58)$$

This weighted version is the correct experimental target, but the unweighted toy version is sufficient for the present executable draft.

## 8 Nuisance-Control and Error Budget

The most serious experimental risk is false covariance. Heating, electromagnetic pickup, flux noise, bias-current drift, device aging, or technical phase noise may create patterns that look residual unless controls are predeclared. Therefore every positive residual claim must survive matched nuisance controls.

A minimal experimental sequence is as follows.

**Protocol 8.1** (Josephson/SQUID residual covariance protocol). For a selected device and temperature regime:

- (JS-1) calibrate the standard SQUID baseline  $I_c^{(0)}(u)$ ;
- (JS-2) measure phase-noise background  $S_{\phi\phi}^{(0)}(\omega; u)$  under ordinary controls;
- (JS-3) run an interleaved flux sweep  $u_i$  with randomized order;
- (JS-4) record  $I_c(u_i)$ ,  $\Gamma_\phi(u_i)$ ,  $\delta\nu_{\text{osc}}(u_i)/\nu_{\text{osc}}$ , and  $S_{\phi\phi}(\omega_0; u_i)$ ;
- (JS-5) subtract or bound heating, pickup, flux-noise, and drift components using Table 2;

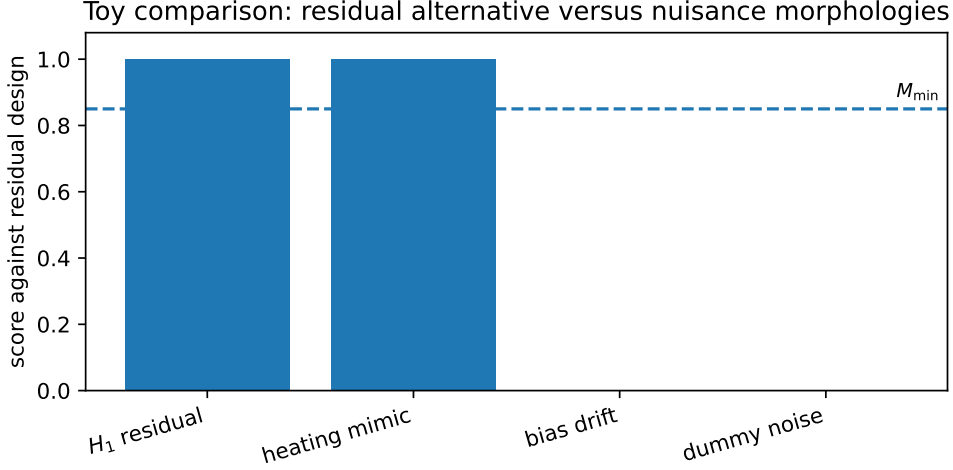


Figure 5: Toy  $H_0/H_1$  morphology comparison. The residual alternative is aligned with the declared design vector by construction, as a positive-control injection. Nuisance morphologies must be tested rather than silently absorbed into the residual ledger.

Table 2: Nuisance-control ledger for the Josephson/SQUID barrier-clock diagnostic.

Nuisance	Control operation	Residual discriminator
Heating	matched power injection; temperature sweep	residual component follows flux geometry rather than heat load
Technical phase noise	dummy resonator; off-resonant channel	absent in a residual-insensitive channel
Electromagnetic pickup	shielding; cable reversal; wiring permutation	does not follow pickup parity or cable geometry
Bias-current drift	interleaved baseline runs; reversed sweep order	no coherent covariance with declared $\mathcal{R}_J(u)$
Flux noise	sign reversal; gradiometric SQUID; repeated flux cycles	predicted $u$ -parity retained after flux-noise subtraction
Device aging	repeated cycles; time-order randomization	secular drift separated from periodic residual morphology
Barrier leakage	subgap leakage monitoring; temperature dependence	residual map does not reduce to leakage current alone

(JS-6) compute morphology scores  $M_k$  against the declared design vector  $g_i$ ;

(JS-7) admit a residual interpretation only if the non-current channels satisfy (57) and sign/parity tests are consistent.

## 9 Falsifiability Ledger

A diagnostic is useful only if it can fail. In the present setting, failure is not merely absence of an exotic signal. It is absence of the specific covariance structure after controls.

**Falsifiability test 9.1** (Current-only failure). If  $I_c(u)$  follows the ordinary SQUID modulation but the non-current channels  $\Delta\Gamma_\phi$ ,  $-\delta\nu/\nu$ , and  $S_{\phi\phi}^{\text{res}}$  do not co-vary with  $\mathcal{R}_J(u)$ , then the residual-clock diagnostic fails. Current modulation alone is ordinary SQUID physics.

**Falsifiability test 9.2** (Nuisance absorption failure). If all candidate residual responses are absorbed by heating, electromagnetic pickup, flux noise, bias-current drift, barrier leakage, or device aging under the controls of Table 2, then no residual interpretation is admitted.

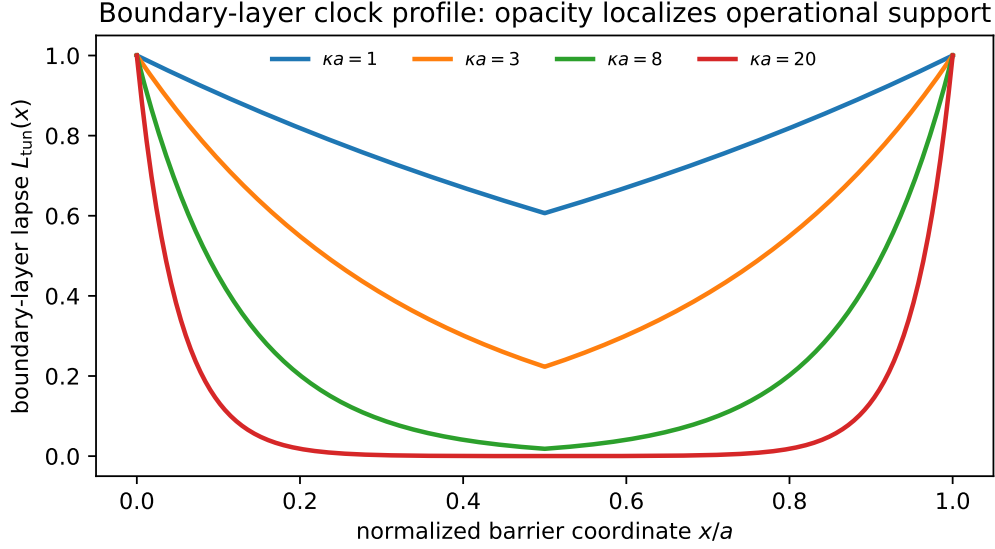


Figure 6: Boundary-layer tunneling clock profile. As  $\kappa a$  grows, the operational support localizes near the two barrier edges. The integral of this support approaches the saturation proxy in (38).

Table 3: Falsifiability ledger for the v0.5 diagnostic.

Test object	Residual-clock success condition	Failure condition
Critical current	only residual correction enters after baseline SQUID fit	raw $I_c(u)$ modulation only
Dephasing	$\Delta\Gamma_\phi(u)$ follows $\mathcal{R}_J(u)$ after controls	dephasing explained by heating or technical noise
Frequency shift	$-\delta\nu/\nu$ has predicted residual parity	drift follows temperature, bias, or time order
Phase-noise spectrum	$S_{\phi\phi}^{\text{res}}(\omega_0; u)$ follows residual morphology	signal appears equally in dummy/off-resonant channel
Tunneling layer	opacity-linked phase-time/noise response survives barrier controls	only transmission changes, no time/noise covariance
Joint admission	at least two non-current channels pass $M_{\min}$	all non-current scores fail

**Falsifiability test 9.3** (Morphology-gate failure). If the morphology scores for all non-current channels fall below the declared threshold,

$$M_\Gamma < M_{\min}, \quad M_\nu < M_{\min}, \quad M_S < M_{\min}, \quad (59)$$

then the tested residual drive  $\mathcal{R}_J(u)$  is rejected for that device and protocol.

## 10 Application Outlook

This note does not propose a commercial device. Its practical value, if the diagnostic is useful, would be in classifying drift and noise in phase-coherent superconducting devices. The most plausible application directions are the following.

**Superconducting qubit decoherence classification.** Josephson junctions are central components of superconducting qubits. A residual-covariance diagnostic could help separate

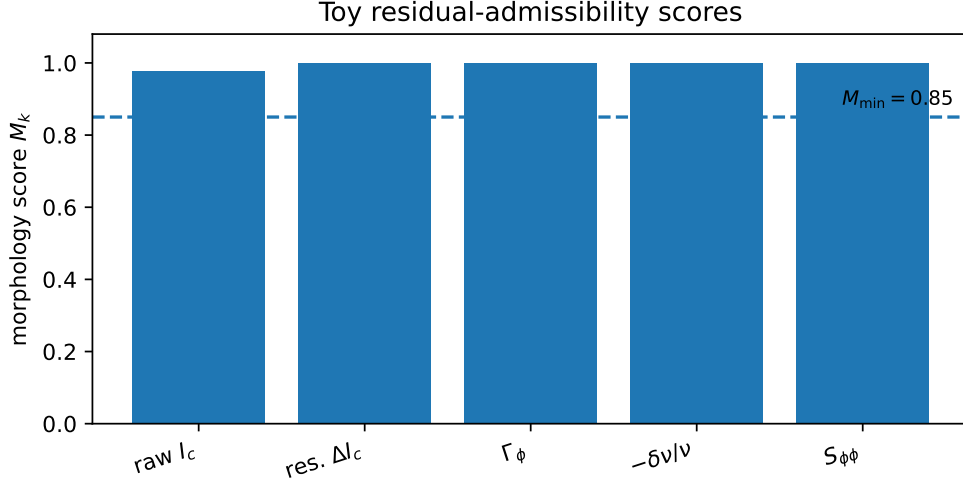


Figure 7: Toy morphology scores. The residual channels pass the illustrative morphology gate by construction because they are positive-control injections. The raw current score is shown only as a caution: ordinary SQUID current modulation is not, by itself, a residual-clock signature.

critical-current fluctuations, phase diffusion, frequency drift, and barrier-related noise into ordinary nuisance classes versus common phase-clock morphology.

**SQUID drift and noise calibration.** SQUID systems are among the most sensitive electromagnetic sensors. A covariance test could improve drift rejection by asking whether a candidate drift follows residual flux geometry or ordinary temperature, cable, pickup, or bias-current controls.

**Tunnel-barrier screening.** Barrier quality is usually assessed through current, leakage, noise, and fabrication uniformity. The barrier-clock layer adds a diagnostic question: does opacity co-vary with phase-time and phase-noise proxies in a way not reducible to leakage or heating?

**Cryogenic RF and quantum metrology.** For low-noise cryogenic electronics and Josephson voltage metrology, the proposed diagnostic may serve as an additional error-budget category. It does not change the voltage standard. It adds a way of asking whether small phase/frequency shifts share a flux-controlled residual morphology.

**High-sensitivity false-positive rejection.** A cross-observable residual score can act as a false-positive rejection rule. A signal that appears only in one channel, or appears equally in a dummy channel, is rejected.

## 11 Conclusion

This v0.5r2 note provides the first executable device-level diagnostic for the Residual Clock–Energy framework. It narrows the broad prediction program to a Josephson/SQUID barrier-clock setting and constructs a toy flux grid, covariance-score rule, boundary-layer tunneling clock proxy, nuisance-control ledger, and falsifiability table.

The main scientific posture is deliberately modest. The note does not claim detection, proof, or a new Josephson law. It proposes a diagnostic architecture:

$$\text{standard Josephson/SQUID baseline} + \text{residual phase-clock covariance test.} \quad (60)$$

The next step is a sensitivity-calibrated v0.6 pass: inject synthetic noise, set plausible thresholds such as  $\Delta\Gamma_{\phi,\min}$ ,  $\Delta(\delta\nu/\nu)_{\min}$ ,  $S_{\phi\phi}^{\min}$ , and  $M_{\min}$ , and test whether the covariance pipeline recovers residual injections after nuisance projection. A complementary v0.6 executable diagnostic based on a CMB TT/TE/EE template grid remains a second candidate.

## A Toy Model Parameters

Table 4: Toy parameters used in the v0.5 executable diagnostic.

Parameter	Meaning	Toy value
$r_0$	residual-drive amplitude	0.05
$\lambda_I$	current correction coefficient	0.2
$\lambda_\nu$	frequency response coefficient	1
$\lambda_\Gamma$	dephasing response coefficient	1
$\lambda_S$	phase-noise response coefficient	1
$\varepsilon_{\text{asym}}$	SQUID visibility smoothing	0.05
$N$	flux-grid resolution	200
$M_{\min}$	illustrative morphology threshold	0.85

These values are not calibrated to a specific device. They are chosen only to make the residual-covariance morphology visible and reproducible. The nuisance comparison curves use schematic constants  $h_0, h_1, q_1, q_2$  only to visualize morphology competition; they are not fitted heating or electronics models.

## B Pseudocode

### Algorithm JSQ-v0.5r2: Toy Josephson/SQUID residual covariance and nuisance grid

Input: flux grid  $u_i = i/N$ , residual amplitude  $r_0$ , coefficients  $\lambda_I, \lambda_\nu, \lambda_\Gamma, \lambda_S$ , smoothing  $\varepsilon_{\text{asym}}$ .

1. Compute  $\mathcal{R}_J(u_i) = r_0 \sin^2(\pi u_i)$ .
2. Compute  $\hat{I}_c^{(0)}(u_i) = \sqrt{\cos^2(\pi u_i) + \varepsilon_{\text{asym}}^2} / \sqrt{1 + \varepsilon_{\text{asym}}^2}$ .
3. Compute  $\hat{I}_c(u_i) = \hat{I}_c^{(0)}(u_i)[1 - \lambda_I \mathcal{R}_J(u_i)]$ .
4. Compute  $\Gamma_\phi(u_i) = \Gamma_0 + \lambda_\Gamma \mathcal{R}_J(u_i)$ .
5. Compute  $\delta\nu_{\text{osc}}(u_i)/\nu_{\text{osc}} = -\lambda_\nu \mathcal{R}_J(u_i)$ .
6. Compute  $S_{\phi\phi}^{\text{res}}(\omega_0; u_i) = \lambda_S F_S(\omega_0) \mathcal{R}_J(u_i)$ .
7. Center  $\mathcal{R}_J$  to obtain  $g_i$ .
8. Compute morphology scores  $M_k$  for residual channels.
9. Admit residual interpretation only if at least two non-current channels pass  $M_{\min}$  after nuisance controls.

## C Relation to the v0.4r1 Public Protocol Note

The v0.4r1 public protocol note, *Prediction and Discriminating Experiments for the Residual Clock–Energy Framework*, DOI [10.5281/zenodo.19846816](https://doi.org/10.5281/zenodo.19846816), organized five diagnostic channels under a cross-channel residual ledger. The present v0.5r2 note is the first one-channel executable diagnostic extracted from that program. Its channel is the combined laboratory phase-clock and quantum tunneling branch:

$$\text{v0.4r1 five-channel protocol} \longrightarrow \text{v0.5 Josephson/SQUID barrier-clock diagnostic.} \quad (61)$$

The purpose is not to replace the broader protocol, but to demonstrate how one channel can be made into a reproducible calculation and falsifiability ledger.

## D Reproducibility Bundle Contents

The accompanying bundle contains the LaTeX source, compiled PDF, figure-generation script, generated figures, and toy flux-grid CSV file. The CSV is not experimental data. It records the toy values used in [Section 6](#) so that the covariance plots and morphology scores can be reproduced or modified.

## References

- [1] B. Lee, *Prediction and Discriminating Experiments for the Residual Clock–Energy Framework*, Version v0.4r1, Zenodo record, 2026. DOI: [10.5281/zenodo.19846816](https://doi.org/10.5281/zenodo.19846816).
- [2] B. Lee, *Operational Time and Residual Energy: A Structural Introduction to Clock–Generator Duality and Gauge–Gravity Response*, Version v1.1, Zenodo record, 2026. DOI: [10.5281/zenodo.19802122](https://doi.org/10.5281/zenodo.19802122).
- [3] B. D. Josephson, *Possible new effects in superconductive tunnelling*, Physics Letters **1**, 251–253, 1962. DOI: [10.1016/0031-9163\(62\)91369-0](https://doi.org/10.1016/0031-9163(62)91369-0).
- [4] M. Tinkham, *Introduction to Superconductivity*, 2nd edition, McGraw–Hill, 1996; Dover reprint, 2004.
- [5] J. Clarke and A. I. Braginski, editors, *The SQUID Handbook. Vol. I: Fundamentals and Technology of SQUIDs and SQUID Systems*, Wiley–VCH, 2004.
- [6] R. L. Fagaly, *Superconducting quantum interference device instruments and applications*, Review of Scientific Instruments **77**, 101101, 2006. DOI: [10.1063/1.2354545](https://doi.org/10.1063/1.2354545).
- [7] W. C. Stewart, *Current-voltage characteristics of Josephson junctions*, Applied Physics Letters **12**, 277–280, 1968.
- [8] D. E. McCumber, *Effect of ac impedance on dc voltage-current characteristics of superconductor weak-link junctions*, Journal of Applied Physics **39**, 3113–3118, 1968.
- [9] K. K. Likharev, *Dynamics of Josephson Junctions and Circuits*, Gordon and Breach, 1986.
- [10] T. E. Hartman, *Tunneling of a wave packet*, Journal of Applied Physics **33**, 3427–3433, 1962.
- [11] M. Büttiker and R. Landauer, *Traversal time for tunneling*, Physical Review Letters **49**, 1739–1742, 1982. DOI: [10.1103/PhysRevLett.49.1739](https://doi.org/10.1103/PhysRevLett.49.1739).
- [12] M. Büttiker, *Larmor precession and the traversal time for tunneling*, Physical Review B **27**, 6178–6188, 1983.
- [13] E. H. Hauge and J. A. Støvneng, *Tunneling times: a critical review*, Reviews of Modern Physics **61**, 917–936, 1989. DOI: [10.1103/RevModPhys.61.917](https://doi.org/10.1103/RevModPhys.61.917).